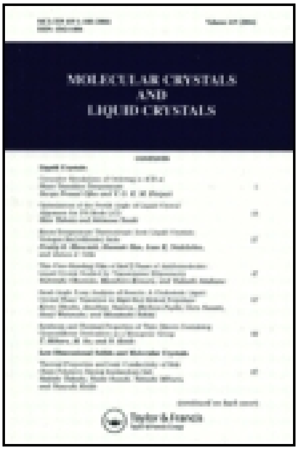

Molecular Crystals and Liquid Crystals

Publication details, including instructions for authors and subscription information:
http://www.tandfonline.com/loi/gmcl16

Phonons in Ideal and "Kinked" Polyacetylene Chains

Eugene J. Mele [a]

[a] Xerox Webster Research Center Webster, New York, 14580

To cite this article: Eugene J. Mele (1981): Phonons in Ideal and "Kinked" Polyacetylene Chains, Molecular Crystals and Liquid Crystals, 77:1-4, 25-41

To link to this article: http://dx.doi.org/10.1080/00268948108075227

Mol. Cryst. Liq. Cryst., 1981, Vol. 77, pp. 25–41
0026-8941/81/7701-0025$06.50/0

Printed in the United States of America

(Proceedings of the International Conference on Low-Dimensional Conductors, Boulder, Colorado, August 1981)

PHONONS IN IDEAL AND "KINKED" POLYACETYLENE CHAINS

Eugene J. Mele*
Xerox Webster Research Center
Webster, New York 14580

Received for publication August 31, 1981

Recent lattice dynamics studies of trans $(CH)_x$ and $(CD)_x$ are reviewed. The calculations employ a force field which describes both the short range covalent bonds and longer range interactions due to indirect couplings through the π electron system. For the ideal chain, the model yields a good description of the long wavelength optical modes observed in Raman scattering. For chains containing a soliton, a spectrum of localized and resonant defect modes is obtained. The optical activity calculated for the soliton provides a remarkably complete description of the reported dopant induced infrared activity in $(CH)_x$ and $(CD)_x$. The effect of a pinning potential on the absorption anticipated in the far infrared is discussed.

INTRODUCTION

The suggestion that trans $(CH)_x$ is a medium which supports stable nonlinear structural excitations or solitons[1,2] has motivated considerable experimental investigation of the magnetic[3], optical[4] and infrared properties[5-7] of doped samples in an effort to identify these defects. In this paper we will briefly review theoretical studies[6,7] which relate to the infrared absorption data on doped films. These studies provide spectroscopic evidence for the presence of bond alternation reversing defects in doped polyacetylene.

MODEL FORCE FIELD FOR POLYENES

To study the vibrational excitations of polyacetylene we have constructed model force field which is composed of two principal parts. First, a short range valence force field is employed to describe the short range covalent forces in the polymer. Second, an extended force field is derived which includes the indirect coupling of carbon motions mediated by the polarization of the π electron gas on the chain.

Short Range Force Field

We have studied the short range covalent forces employing both a Born Hamiltonian[8] and a Keating Hamiltonian.[9] Although our initial studies employed the simpler Born model, the Keating parameterization provided an improved description of the vibrations in both $(CH)_x$ with a single set of force constants and was consequently adopted in all subsequent calculations. The Keating Hamiltonian is the simplest short range force field one can construct which both includes noncentral bond bending forces and is invariant under rotation. The Keating model assigns to every nearest neighbor bond between sites i and j in the solid a harmonic bond stretching potential:

$$V_{bs} = \frac{1}{2} K_s \left(\vec{x}_{ij} \cdot \vec{x}_{ij} - \vec{u}_{ij} \cdot \vec{u}_{ij} \right)^2 / |\vec{u}_{ij}|^2 \qquad (1)$$

where x_{ij} is the instantaneous vector from site i to site j and u_{ij} is the equilibrium value of x_{ij}. The bond bending potential for the bond angle between x_{ij} and x_{ik} is written:

$$V_{bb} = \frac{1}{2} K_b \left(\vec{x}_{ij}\cdot\vec{x}_{ik} - \vec{u}_{ij}\cdot\vec{u}_{ik}\right)^2 / |\vec{u}_{ij}|^2 |\vec{u}_{ik}|^2 \qquad (2)$$

For $(CH)_x$ we thus have five independent parameters: K_s(C-C), K_s (C=C), K_s (C-H), K_b (CCC) and K_b (C-CH) ≡ K_b (C=CH). These constants are assigned values estimated from the vibrational frequencies of the small organic molecules: C_2H_6, C_2H_4, C_3H_6 and C_6H_6.[10] One subtle aspect to this choice of force constants is noteworthy. The sigma electron contributions to the C-C stretching force constants are plotted in Figure 1 as a function of bond length.[11] The plot shows that the sigma force constant itself changes by more than a factor of two over the range of bond lengths spanning the double bond in ethylene to the single bond in ethane. Since we expect bonds of intermediate length in $(CH)_x$

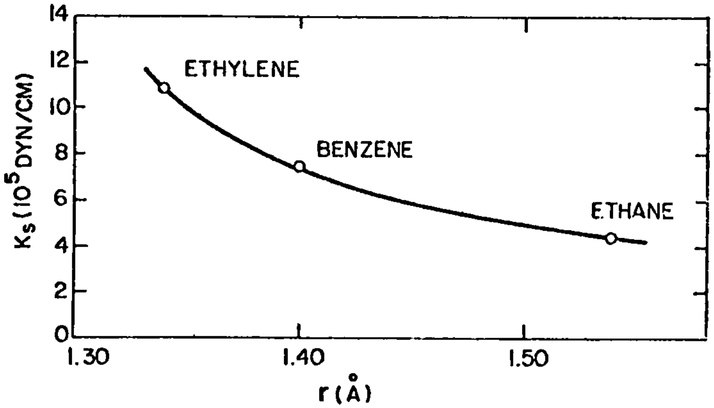

Figure 1. Sigma spring constant for carbon-carbon bond as a function of bond length.

(estimated 1.36A and 1.43A)[12], the values of K_S are interpolated along the curve given. This procedure yields the set of force constants tabulated in Table 1. Most current studies adopt the spring constant of ethane for work on $(CH)_X$, ignoring the anharmonicity in Figure 1. The consequences of this choice are apparently an overestimate of the bond alternation amplitude or an underestimate of the electron phonon coupling strength.

Table 1. Keating Hamiltonian Parameters for $(CH)_X$

K_S (C=C = 8.88×10^5 dyn/cm

K_S (C-C) = 6.70×10^5 dyn/cm

K_S (CH) = 5.15×10^5 dyn/cm

K_b (CCC) = 1.99 mdyn A/rad^2

K_b (CCH) = 0.84 mdyn A/rad^2

Long Range Force Field

The polarization of π electron states on the polymer backbone gives rise, in addition, to an extended force field in the molecule. This effect can be derived simply in second order perturbation theory. Assume the π electron Hamiltonian is expanded to linear terms in the atomic displacements:

$$\mathcal{H} = \mathcal{H}^{0} + \sum_{\mu} \vec{V}_{\mu} \cdot \vec{\delta x}_{\mu} \qquad (3)$$

In the adiabatic approximation the ground state expectation value of H includes a term second order in the x :

$$E^{(2)} = \frac{1}{2}\sum_{\mu\nu} -\vec{\delta x}_{\mu}^{*}\left[2\sum_{\substack{n<\\n'>}} \frac{\langle n|V_{\mu}^{*}|n'\rangle\langle n'|V_{\nu}|n\rangle}{E_{n'}-E_{n}}\right]\vec{\delta x}_{\nu} \tag{4a}$$

$$= \frac{1}{2}\sum_{\mu\nu} \vec{\delta x}_{\mu}^{*}\cdot K^{\pi}_{\mu\nu}\cdot \vec{\delta x}_{\nu} \tag{4b}$$

Though the π electron contribution to the dynamical matrix, $K^{\pi}{}_{\mu\nu}$, has long been known to be important for lattice dynamics in polyenes[13], explicit calculation for finite sytems is computationally involved.[11,14] Fortunately, the periodicity of the ideal infinite chain makes direct calculation of $K^{\pi}{}_{\mu\nu}$ more tractable;[15] in Figure 2 we show our results for the longitudinal terms in $K^{\pi}{}_{\mu\nu}$, plotted as a function of the separation of the sites μ and ν. The force field is oscillatory and decaying with the range of the interaction extending over roughly six nearest neighbors. In our calculations in $(CH)_X$ the magnitude of $V\mu$ in (3) is empirically adjusted to give the best overall fit to the long wavelength optical modes as seen by Raman scattering.[16-18] Only the deformation potential is adjusted in this model as we assume fixed representative values for the other important quantities in the theory (bond lengths: 1.36A and 1.43A, CCC bond angle: 120 , and mean transfer integral: 3 eV). In the fitting procedure, the electronic excitation spectrum and hence $K^{\pi}{}_{\mu\nu}$ are of course recalculated for each trial value of $V\mu$. The deformation potential thus derived ($\partial t/\partial u$, where u is the bond length and t the transfer integral) is 8 eV/A.

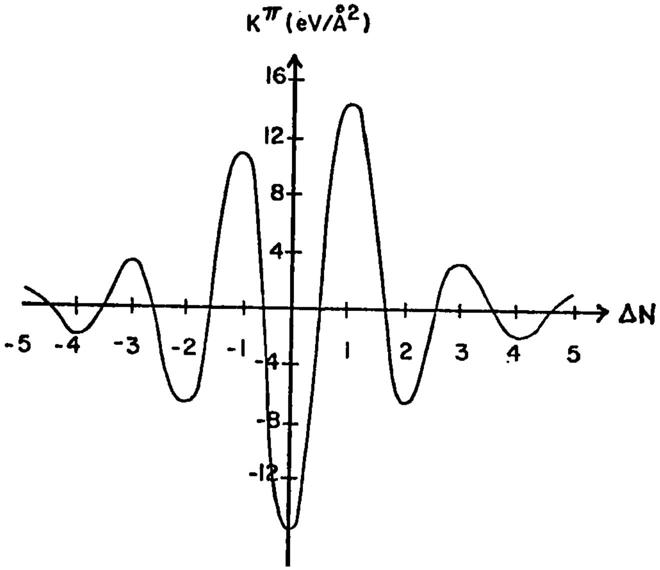

Figure 2. π-electron force field for longitudinal carbon motions in polyacetylene.

Trans $(CH)_x$ and - $(CD)_x$: Ideal Chains

The calculated in plane vibrations for infinite ideal trans $(CD)_x$ and $(CD)_x$ chains are given in Figure 3. In both systems we obtain four optical bands of mixed skeletal stretching and sidegroup bending character. The strong overbending of the highest optical band is a consequence of the extended force field described above.[15] Though each structure has three long wavelength Raman active A_g modes below 2000 cm^{-1}, the associated Raman intensities, which are found to be proportional to the squares of the longitudinal stretching components of these vibrations, difffer greatly. Specifically, only the lowest and highest lying A_g modes (labelled s) in $(CH)_x$ are observably Raman active, while all three A_g modes in $(CD)_x$ are accessible in Raman scattering. This remarkable isotope effect has been reported

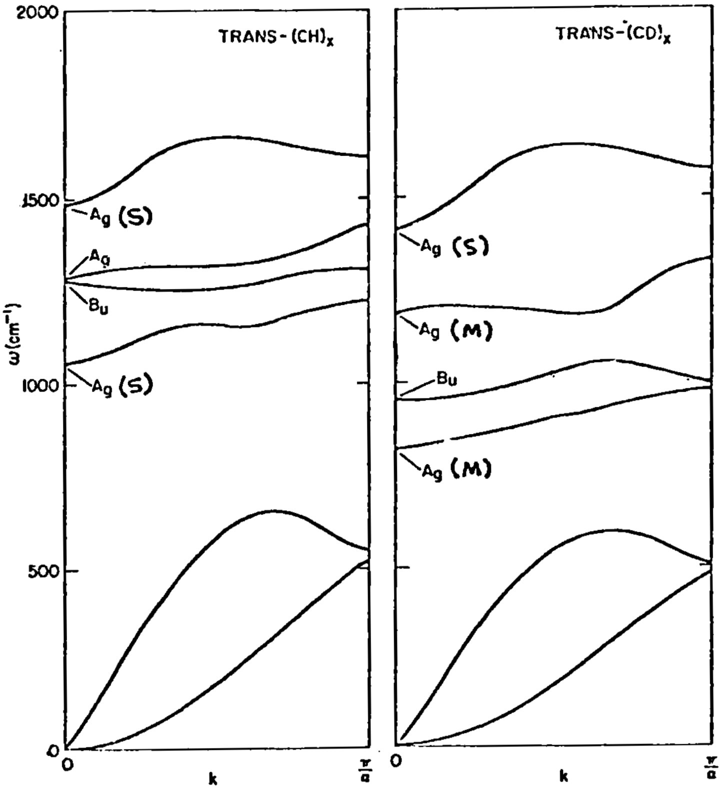

Figure 3. In plane phonons below 2000 cm^{-1} in trans (CH)$_x$ and (CD)$_x$.

experimentally.[19] The lower two acoustic bands in the two structures are dominated by skeletal bending motions. Thus they are only very weakly coupled to the π electrons.

APPLICATION TO SOLITONS

Application of this model to a soliton in a polyene chain is reasonably straightforward. We proceed by assuming that a stable distortion of the chain exists which inverts the bond alternation amplitude u(x) across a length l:[1,2]

$$u(x) = u \tanh((x-x_0)/l) \qquad (5)$$

In the presence of this distortion, the short range force field is immediately calculable. Further, we calculate the π electronic spectrum in the presence of the kink, from which the excitation spectrum and hence the new $K^{\pi}{}_{\mu\nu}$ (eq. 4a) is explicitly evaluated. The fermi factors in equation 4a are chosen to describe a negatively charged kink so that the midgap soliton level is full (there is electron-hole symmetry in the model so that the same result applies to the positively charge defect). The decay length, *l*, is taken to be 5 bond lengths in these calculations. Explicit verification of the stability of the distortion (eq. 5) is beyond the scope of the present calculations; however, the form of the distortion is anticipated from previous model theories[1,2] and our approach should give a good description of the effect of this type of defect on the vibrational structure. Finally the kink is a periodicity breaking distortion on the chain; to evaluate the local vibrational structure we perform a calculation on a finite 15 carbon atom length of chain in which solutions are matched at the boundaries to propagating or decaying solutions for the defect free chain.[6] The calculation thus employ a Green's function formalism in which the presence of the infinite system is induced through an "effective field" or complex frequency dependent self energy. The details of this approach will be presented at a later time. All properties of interest; i.e., densities of states and response functions, are calculable from the full Green's function in the finite segment.

In Figure 4 we compare the carbon site local density of modes obtained for the ideal chain (dashed curve) with that obtained for the chain containing a kink (solid curve). The two curves differ significantly. The defect localizes five well defined internal vibrations either as bonafide local modes or as well defined resonances. These localized vibrations originate from the adjacent higher lying continua. The downshift in frequency is dominantly a consequence of the increased strength of the $K^{\pi}_{\mu\nu}$ (equation 4) due in turn to the presence of the midgap electronic level in the soliton.

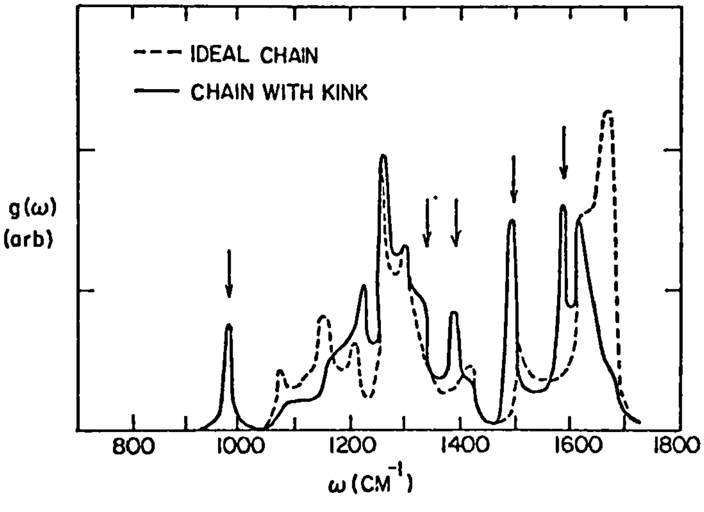

Figure 4. Local densities of states for carbon motions in ideal $(CH)_X$ (dashed) and a soliton in $(CH)_X$ (solid).

INFRARED ACTIVITY OF CHARGED KINKS

While the internal vibrational structure of the soliton is quite complicated (Figure 4), a more useful quantity of experimental interest is the frequency dependent conductivity associated with this spectrum. To investigate this property we study the coupling of the full vibrational spectrum of the soliton (local modes, resonances and continuum solutions) to current fluctuations in the π electron gas. The calculations follow the lines described in reference 20, and amount to computation of the dynamic charge in the system in a formulation similar to equation 4a in which one electron-phonon vertex is replaced by the dipole matrix element (electron-photon coupling). Importantly, this contribution vanishes for a neutral chain (one π electron per site), independent of the structure. Thus the calculated infrared activity is completely due to the excess charge on the polymer.

The results of this calculation for a soliton in a $(CH)_X$ chain and a $(CD)_X$ chain are shown in Figure 5 and compared with experiment. For $(CH)_X$ we obtain two strongly infrared active modes near 980 cm^{-1} and 1390^{-1}. The oscillator strengths are enormous so that moderately low dopant levels ($\sim10^{18}$-$10^{19}cm^{-3}$) this absorption would be experimentally observable. As shown with the dashed curve, the absorption obtained theoretically is well correlated with the absorption obtained by subtraction of infrared absorption spectra before and after doping. Normalized to a uniform doping density, the integrated experimental absorption is of the same order of magnitude as the theoretical result, though the theory overestimates the integrated strength in these features by nearly a factor of three.

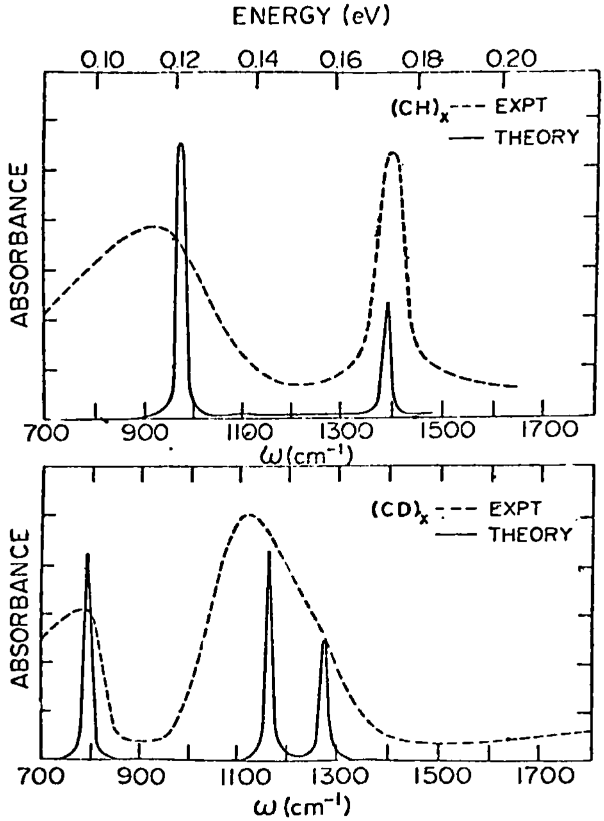

Figure 5. Theoretical (solid line) and experimental (dashed line) absorption profiles for charged solitons in $(CH)_x$ and $(CD)_x$.

The experimental dopant induced infrared absorption spectrum undergoes dramatic alteration upon deuteration as shown in the lower panel.[7] Remarkably the theoretical absorption is also qualitatively modified by deuteration, with three principle features found at 790 cm^{-1}, 1160 cm^{-1} and 1270 cm^{-1}. The theory thus accounts for the apparent broadening of the upper feature seen experimentally and the transfer of oscillator strength from the lower to the upper feature upon deuteration. This remarkable effect is not due to a fundamental change is symmetry between the two structures, but is rather a quantitative effect resulting from unequal distribution of oscillator strengths into various components of the soliton vibrational spectrum.

In fact, the number of strong infrared features obtained for these defects is well correlated with the number of A_g modes which are strongly Raman active in the ideal chains. This is not an accident, since strong Raman activity results from strong coupling to band edge π electronic excitations, hence these vibrational bands are most severely affected by the excess screening from the midgap defect level in the soliton. This yields, for each such coupled band, a localized antisymmetric defect mode with efficient coupling to the conduction charge and hence a large absorptivity.

A point of controversy has arisen concerning whether the infrared activity might be due to the extended crystalline A_g modes perturbed by some point defect induced by doping.[21,22] If the defect envisoned does not reverse the bond alternation amplitude then the mechanism appears unlikely. In a normal mode analysis one could decompose such a perturbed "A_g" mode into the original A_g vibration and a weak admixture of the B_u modes in the system, the mixing due to the perturbation. The infrared response for this mode would then be second order in the perturbation, presumably two weak to be compatible with the strong observed absorption. If the defect envisioned does reverse the bond alternation of the chain one recovers a description very close to the soliton picture described above. Here the defect would fundamentally (not perturbatively) modify the symmetry properties of the chain; each long wavelength A_g mode would be replaced by an A_1 (symmetric) and B_1 (antisymmetric) mode, with the latter mode possessing strong infrared activity polarized along the chain. This is qualitatively the picture for the soliton in polyacetylene. However, even here, this description should not be taken very literally, as it would apply only if the A_1-B_1 splitting were weak with the resulting B_1 mode weakly localized so it could be described as an A_g mode gradually changing phase through the defect. In fact normal coordinate analysis for the infrared active vibrations shown in Figure 5 show rather strong localization of the vibrations to the defect. Further, the perturbation due to the soliton is so strong that there appears to be mixing of the character of the various coupled A_g bands in each localized vibration. Thus the infrared active modes are best described as local vibrations of the soliton. A picture of a crystalline A_g mode rendered antisymmetric in the field of a bond alternation reversing defect is a qualitatively correct description of this phenomena. A model which does not involve reversal of bond alternation would appear inconsistent with the data.

OPTICAL ACTIVITY IN THE FAR INFRARED

The calculations described above have been parameterized and carried out for a soliton at a fixed position on a $(CH)_x$ chain. However due to the translational invariance of the choice of origin for this system we anticipate an additional zero frequency (Goldstone) mode associated with the translation of the defect in the chain. The kinematical parameters describing the translation of a soliton on a $(CH)_x$ chain have been worked out in several theoretical studies, yielding a general concensus[2,23] about the inertial mass ($\sim m_e$) charge (e) and pinning frequency in a coulomb well for this defect ($\sim 300\ \mathrm{cm}^{-1}$). Though measurable infrared activity in this spectral range due to doping has been expected, none has been observed.[22,24]

There are two noteworthy explanations for this discrepancy. The first has been proposed in a recent paper by Horowitz[25] who suggests that the lower mode observed experimentally is in fact the pinning mode. The suggestion leaves open the question of the orgin of the tremendous theoretical underestimate of the pinning frequency (almost an order of magnitude error in the restoring force), and further, is difficult to reconcile with the normal coordinate calculated for the lower infrared active defect mode. However, it does resolve the absence of absorption in the far infrared.

A second, and more likely, resolution involves a breakdown of the "rigid translation" hypothesis which underlies the present theoretical estimates. Present studies derive kinematical parameters for the kink, assuming that the pinning oscillation of the defect can be modelled by rigidly translating the defect on the chain. This is reasonable so long as the pinning frequency is much smaller than any internal excitation energy in the defect, and would apply, for example, if the defect were condensed entirely from optical phonons, which all lie at rather high frequency in this system (interestingly, this assumption appears to be reasonable in a linear chain approximation). We believe the rigid motion picture breaks down in $(CH)_x$ due to a nonzero (albeit weak) coupling of the acoustic bands to the π electrons. We anticipate such coupling for two reasons. First, it is not symmetry forbidden and indeed probably even occurs in the present simple model for $(CH)_x$. Second, the formation of a defect which changes both bond lengths on a zigzag chain will leave the length of the system invariant only if either the displacements are constrained to lie along the chain, or if there is a compensating modulation of the CCC bond angles. The latter is anticipated in any real system and implies electronic coupling in the acoustic band. We have carried out calculations[26] which indicate that when the pinning frequency becomes comparable to or larger than the frequency of the lowest coupled mode, oscillator strength is suppressed in the "pinning" mode and reappears in the conductivity of the higher lying phonons. A suppression of the sliding mode oscillator strength by nearly two orders of magnitude with this mechanism is quite possible for a pinning strength as weak as $300\mathrm{cm}^{-1}$. Details of these studies will be forthcoming.[26]

ACKNOWLEDGMENTS

The work discussed above has been carried out in collaboration with M.J. Rice. We are grateful for experimental support from S. Etemad and A.J. Heeger, and to B. Horowitz for a stimulating preprint.

*Permanent Address: Dept. of Physics, University of Pennsylvania, Philadelphia, PA 19104.

REFERENCES

1. M.J. Rice, Phys. Lett. 71A, 152 (1979).
2. W.P. Su, J.R. Schrieffer, and A.J. Heeger, Phys. Rev. Lett. 42, 1698 (1979).
3. S. Ikehata, J. Kaufer, T. Woerner, A. Pron, M.A. Dry, A. Sivak, A.J. Heeger and A.G. MacDiarmid, Phys. Rev. Lett. 45, 1123 (1980).
4. N. Suzuki, M. Ozaki, S. Etemad, A.J. Heeger and A.G. MacDiarmid, Phys. Rev. Lett. 45, 1209 (1980).

5. C.R. Fincher, M. Ozaki, A.J. Heeger and A.G. MacDiarmid, Phys. Rev. B19, 4140 (1979).

6. E.J. Mele and M.J. Rice, Phys. Rev. Lett. 45, 926 (1980).

7. S. Etemad, A. Pron, A.J. Heeger, A.G. MacDiarmid, E.J. Mele and M.J. Rice, Phys. Rev. B.

8. M. Born, Ann. Phys. 44, 605 (1914).

9. P.N. Keating, Phys. Rev. 145, 637 (1966).

10. See e.g. G. Herzberg, Infrared and Raman Spectra of Polyatomic Molecules, Van Nostrand, New York (1945).

11. T. Kakitani, Prog. Th. Phys. 51, 656 (1974).

12. J. Bart and C.H. MacGillvary, Acta Crystallographica B24, 1569 (1968).

13. C.A. Coulson and H.C. Longuet Higgins, Proc. R. Soc. London A193, 457 (1948).

14. R.M. Gavin and S.A. Rice, J. Chem. Phys. 55, 1675 (1971).

15. E.J. Mele and M.J. Rice, Solid State Comm. 34, 339 (1980).

16. I. Harada, M. Tasumi, H. Shirikawa and S. Ikeda, Chem. Lett. 1411 (1974).

17. S. Lefrant, L.S. Lichtmann, H. Temkin and D.B. Fitchen, Solid State Comm. 29, 191 (1979).

18. M. Kuzmany, Phys. Stat. Sol. 91, 521 (1980).

19. L.S. Lichtmann, A. Sarhangi and D.B. Fitchen, Solid State Comm. 36, 869 (1980).

20. H.J. Schulz, Phys. Rev. B18, 5756 (1978).

21. J.F. Rabolt, T.C. Clarke and G.B. Street, J. Chem. Phys. 71, 4614 (1979).

22. J.F. Rabolt, T.C. Clarke and G.B. Street, Bull. Am. Phys. Soc. 26, 347 (1980).

23. M.J. Rice and E.J. Mele, Solid State Comm. 35, 487 (1980).

24. D.M. Hoffman, D.B. Tanner, A.J. Epstein and H.W. Gibson, Bull. Am. Phys. Soc. 26, 345 (1981).

25. B. Horowitz (preprint 1981).

26. E.J. Mele and M.J. Rice (unpublished results).